Hartree-Fock calculations for crystalline Ne and LiF

R. N. Euwema , G. G. Wepfer, G. T. Surratt, and D. L. Wilhite*
Aerospace Research Laboratories, Wright-Patterson Air Force Base, Ohio 45433
(Received 9 November 1973)

The self-consistent Hartree-Fock energy bands which are presented in this paper for LiF and Ne closely match Hartree-Fock energy bands reported by other groups for these compounds. The Hartree-Fock equilibrium lattice constant and bulk modulus for LiF are 3.972 Å and 7.54×10^{11} dyn/cm^2, as compared to the experimental values of 4.02 Å and 6.71×10^{11} dyn/cm^2. Hartree-Fock x-ray structure factors and directional Compton profiles in the impulse approximation are presented. The calculated x-ray structure factors of LiF agree with experiment to within 2%, while the calculated Compton profiles of LiF agree with experiment to within 3%.

I. INTRODUCTION

In previous papers, we presented a straightforward crystal Hartree-Fock (HF) formalism which utilizes crystalline symmetry and various two-electron integral approximations.[1] Diamond results were given for energy bands, the cohesive energy, and x-ray structure factors[1]; for the HF equilibrium lattice constant and bulk modulus[2]; and for directional Compton profiles calculated in the impulse approximation.[3] These results suggest that correlation is not a major factor in the ground-state properties, except for the cohesive energy, but is very important in the description of the energy bands.

In the present paper, a slightly improved HF computational model is applied to crystalline Ne and LiF. These compounds were chosen partly because HF energy bands have already been calculated for these materials with Gilbert's local-orbital (LO) formalism by Kunz and Mickish,[4,5] and with a muffin-tin augmented-plane-wave (APW) formalism by Dagens and Perrot.[6,7] Our energy bands can thus be compared to these earlier results. The results for ground-state energetics and for the first-order density matrix (as measured by Compton profiles and x-ray structure factors) are compared to experimental results for LiF, and are presented for future comparison with experimental results for Ne.

II. COMPUTATIONAL DETAILS

Our basic canonical HF formalism is discussed in detail in Ref. 1. Contracted sets of Gaussians centered on atom sites are used as local basis functions

$$\varphi_s(\vec{r}) = \sum_\alpha A_\alpha e^{-\alpha r^2}$$

together with Gaussian lobe functions of p symmetry

$$\varphi_p(\vec{r}) = \sum B_\alpha (e^{-\alpha(\vec{r}-\vec{R})^2} - e^{-\alpha(\vec{r}+\vec{R})^2}) \approx \sum B_\alpha e^{-\alpha r^2}(-4\alpha \vec{r}\cdot\vec{R}).$$

These functions consist of oppositely signed Gaussians with centers slightly displaced in order to simulate Cartesian Gaussians. The contracted sets of Gaussians used in this study are given for Ne in Table I and for LiF at the experimental lattice constant in Table II. The corelike basis functions were taken from tables compiled by Huzinaga[8] for the free atom, while the more diffuse Gaussians were adjusted to minimize the total energy of the crystal, and to lower the conduction eigenvalues.

The local basis functions are used to construct Bloch basis functions at a regular mesh of 19 inequivalent points in the first Brillouin zone

$$\Phi_\mu^k(\vec{r}) = \sum_a e^{i\vec{k}\cdot\vec{R}_a}\varphi_\mu(\vec{r}-\vec{R}_a).$$

The local basis functions also form a basis for the first-order density matrix

$$\rho_1(\vec{r},\vec{r}\,') = \sum A_{\mu\nu}^{ab}\varphi_\mu(\vec{r}-\vec{R}_a)\varphi_\nu^*(\vec{r}\,'-\vec{R}_b).$$

Varying the coefficients of the Bloch basis functions to minimize the total crystalline energy then leads to the usual matrix eigenvalue-eigenvector problem for each zone point

$$H^k\Psi_i^k = \lambda_i^k U^k \Psi_i^k,$$

$$H_{\mu\nu}^k = \left\langle \Phi_\mu^k(\vec{r}) \middle| -\nabla^2 - \sum_a \frac{2Z_a}{|\vec{r}-\vec{R}_a|} + \int d(\vec{r}\,') \frac{2\rho_1(\vec{r}\,',\vec{r}\,') - \rho_1(\vec{r},\vec{r}\,')P_{rr'}}{|r-r'|} \middle| \Phi_\nu^k(r) \right\rangle,$$

$$U_{\mu\nu}^k = \langle \Phi_\mu^k(\vec{r}) | \Phi_\nu^k(\vec{r}) \rangle,$$

where $P_{rr'}$ interchanges variables r and r'.

The secular equation is solved using the Löwdin

TABLE I. Gaussian basis for Ne. The coefficients C multiply normalized $1s$ and $2p$ Gaussians, $Ce^{-\alpha r^2}$. Atomic units are used throughout.

	α	C		α	C
$1s$	47 870.213	0.000 209 549	$1p$	84.8396	0.036 158 526
	7355.8349	0.001 616 522		19.7075	0.239 481 67
	1660.1762	0.008 611 477		6.218 77	0.811 942 44
	460.538 77	0.036 244 592	$2p$	2.160 902 2	0.447 095 37
	146.038 08	0.122 191 475		0.705 515 92	0.503 568 3
	50.413 86	0.307 653 162	$3p$	0.34	1
$2s$	18.279 945	0.712 234 4	$4p$	0.15	1
	6.707 072 1	0.325 45			
$3s$	1.924 453 9	0.385 495 36			
	0.720 813 21	0.524 560 63			
$4s$	0.3	1			
$5s$	0.13	1			

orthogonalization procedure.[9] We use this technique to eliminate linear dependence in the following manner: The eigenvalues of the overlap matrix are scaled so that the largest eigenvalue is unity. The eigenvectors corresponding to scaled eigenvalues less than some tolerance (typically 0.005–0.01) are discarded. The Hamiltonian matrix is then transformed with the remaining rectangular matrix in the usual manner. We will return to the choice of the overlap tolerance later.

The eigenfunctions for the filled electron states are used to build new first-order density matrix coefficients $A_{\mu\nu}^{ab}$ at each of the 19 zone points. These coefficients are then averaged with appropriate weights to obtain the updated first-order density matrix, which in turn yields an updated Hamiltonian. The process is iterated to self-consistency.

Crystalline symmetry is used to reduce the number of integrals which must be done, and to combine the integrals before entering the self-consistent cycle. These techniques are fully described in Ref. 1. In addition, three charge-conserving integral approximations are used. These permit us to zero or approximate all of the smaller, relatively unimportant integrals without destroying the very important balance between nuclear and electronic charge. These procedures are summarized in the Appendix. The tolerances given in parentheses in the Appendix were used in this study.

In our first two papers,[1,2] we only calculated two-electron integrals for which all four local basis functions were within six shells of neighbors of each other. To compensate for this sharp cutoff at the computational boundary, we introduced so-called monopole and dipole corrections. We no longer need these corrections, because we now calculate integrals over many more shells of

TABLE II. Gaussian basis for LiF for the lattice constant 4.018 52 Å. For notation and units, see Table I.

	Li			F	
	α	C		α	C
$1s$	1354.9159	0.000 847 312	$1s$	10 255.863	0.001 129 262
	203.301 16	0.006 513 912		1545.5575	0.008 586 802
	46.323 493	0.032 726 414		357.069 77	0.041 957 136
	13.133 489	0.118 486 46		103.631 43	0.146 491 37
	4.247 754 2	0.296 433 8		34.502 616	0.351 911 32
	1.487 274 3	0.447 232 88		4.831 832 8	0.158 194 61
$2s$	0.6	1	$2s$	12.546 095	1
$3s$	0.3	1	$3s$	1.233 123 5	1
$1p$	0.3	1	$4s$	0.6	1
			$5s$	0.24	1
			$1p$	44.608 007	0.016 248 533
				10.096 673	0.102 196 15
				2.984 881 3	0.312 641 05
			$2p$	0.93	1
			$3p$	0.27	1

TABLE III. HF energy bands of Ne in Ry. The LO results are from Ref. 4. The APW results are from Ref. 6. All results are adjusted in absolute position so that Γ_{15} is at 0.0 Ry.

	Present calc.	LO	APW
1s	−63.879	−63.927	−63.854
$\Gamma_1(2s)$	−2.178	−2.190	−2.176
Γ_{15}	0	0	0
Γ_1	1.882	1.846	1.868
$\Gamma_{25'}$	3.822	4.101	3.201
$X_1(2s)$	−2.173	−2.183	···
$X_{4'}$	−0.044	−0.022	−0.034
$X_{5'}$	−0.017	0	−0.012
$X_{4'}$	2.438	2.448	2.420
X_1	2.670	2.822	2.348
$X_{5'}$	3.016	3.139	2.983
$L_1(2s)$	−2.175	−2.176	···
$L_{2'}$	−0.048	−0.029	−0.036
$L_{3'}$	−0.006	0	−0.019
$L_{2'}$	2.288	2.279	2.254
L_1	2.372	2.417	2.315
$L_{3'}$	3.571	3.778	3.084

neighbors, and then use Ewald summation techniques to handle the remaining infinite crystal.[10]

III. ENERGY BANDS

Our HF energy bands are given for Ne in Table III and for LiF in Table IV. The LO and APW HF bands are also given. For ease of comparison, the top valence band at Γ has been set to zero in each case. [No information is lost by this adjustment of the levels. The zero of potential, and hence the absolute positions of the energy eigenvalues, is dependent upon the (arbitrary) grouping of positive and negative charge contributions to the conditionally convergent summation.] One word of caution is in order. Our HF eigenfunctions have not been symmetry analyzed. Present symmetry assignments are based upon the degeneracy of the eigenvalues, and upon their agreement with the earlier published results. This procedure is dangerous for the higher conduction bands.

TABLE IV. HF energy bands for LiF in Ry. The LO results are from Ref. 5. The APW results are from Ref. 7. These results are adjusted in absolute position so that Γ_{15} is at 0.0 Ry. The Li and F 1s levels are also given.

	Present calc.	LO	APW
F 1s	−51.333	−51.85	···
Li 1s	−3.617	−3.62	···
Γ_1	−1.892	−2.021	···
Γ_{15}	0	0	0
Γ_1	1.685	1.688	1.552
Γ_{15}	2.870	3.188	2.692
X_1	−1.844	−1.886	···
$X_{4'}$	−0.245	−0.259	−0.149
$X_{5'}$	−0.088	−0.081	−0.055
X_3	2.211	2.478	2.001
X_1	2.352	2.493	2.077
$X_{5'}$	2.610	2.906	2.523
L_1	−1.895	−1.924	···
$L_{2'}$	−0.220	−0.223	−0.138
$L_{3'}$	−0.022	−0.033	−0.018
L_1	1.819	1.847	1.733
$L_{2'}$	2.428	···	2.117
L_3	2.495	2.700	2.427

The agreements between the three sets of calculations is striking for the core levels, the valence bands, and the lowest conduction bands. This agreement is especially impressive when it is remembered that completely different computational formalisms were employed by the three research groups.

Comparison of the higher conduction bands shows a shortcoming of the analytic local basis functions. The conduction-band wave functions are large in the interstitial regions. Our calculations, and those of the LO formalism, both suffer from inadequate basis sets in these regions. The APW muffin-tin potential does not handle the interstitial regions correctly either, so these higher conduction bands are also suspect.

The close agreement of our results with those of the other groups for the lower bands for both the rare-gas crystal Ne and for the ionic crystal LiF gives us confidence that our Ewald summation technique and various integral approximations are sound.

Both of the other research groups have applied correlation corrections to the HF energy bands and have obtained close agreement of the corrected bands with experiment. In this paper, we shall concentrate upon ground-state properties.

IV. GROUND-STATE ENERGETICS

We performed LiF calculations at five separate lattice constants. The standard deviations of the outer overlapping Gaussians were scaled directly with the lattice constant. The Gaussian with an exponent of 0.93 was only partially scaled. The essentially nonoverlapping core basis functions describe the behavior of the crystal wave functions in the vicinity of the nuclei, and should consequently not be scaled. The Gaussian exponent coefficients that were scaled are tabulated in Table V for the five LiF lattice constants.

Table VI gives the total energy per atom for Ne and the total energy per atom pair for LiF for

TABLE V. LiF Gaussian exponent coefficients in a.u. for five lattice constants (in Å).

		3.82	3.90	4.018 52	4.10	4.20
Li	2*s*	0.663 98	0.637 022	0.6	0.576 389 2	0.549 27
	3*s*	0.331 99	0.318 511	0.3	0.288 194 6	0.274 635
	1*p*	0.331 99	0.318 511	0.3	0.288 194 6	0.274 635
F	4*s*	0.663 98	0.637 022	0.6	0.576 389 2	0.549 27
	5*s*	0.265 593	0.254 808 7	0.24	0.230 555 7	0.2197
	2*p*	0.98	0.955	0.93	0.91	0.90
	3*p*	0.298 79	0.286 659 8	0.27	0.259 375	0.247 17

each lattice constant. The atomic HF total energies are also given for the atomic Gaussian bases. The comparison of results from two calculations done with different basis sets is not altogether valid. However, in the present case there is no alternative.

For ionic crystals such as LiF, there are two commonly used definitions of binding energy. One definition is "the energy required per pair to construct the crystal from individual isolated free atoms." Experimentally,[11] this value is 0.69 Ry/pair, while our HF value is 0.53 Ry/pair. It is hard to estimate how much of the difference is due to correlation and how much is due to a poor Gaussian basis. The crystal Gaussian basis has an important deficiency. The Gaussian contractions appropriate to free atoms were used, whereas in retrospect it would have been better to use contractions appropriate to the Li^+ and F^- ions.

The more usual definition of binding energy for ionic crystals refers to "the energy required per pair to construct the crystal from individual isolated Li^+ and F^- ions." To calculate the HF energy of the free ions, we performed restricted HF calculations on the ions, using the same contracted basis sets as were used in the crystal, together with some additional longer-range Gaussians. We obtained a HF ionic binding energy of 0.82 Ry/pair, which should be compared to the experimental value[12] of 0.79 Ry/pair. We suspect that this agreement is fortuitously close. Löwdin,[9] in a much earlier non-self-consistent HF calculation of LiF obtained 0.71 Ry/pair for the ionic binding. Froman and Löwdin[13] have given arguments that the correlation corrections to the ionic binding should be very small. Our results are consistent with their conclusions.

The results for neon are given in Table VI for two choices of the overlap tolerance. For an overlap tolerance of zero, one obtains a nonphysical binding of 0.019 Ry/atom, while for an overlap tolerance of 0.014 the crystal is unbound by 0.0037 Ry/atom. Rare-gas crystals are thought to be unbound in the HF approximation,[14] and the experimental binding energy[15] is only 0.0019 Ry/atom. This would seem to indicate that the tolerance of 0.014 is in some sense more correct. However, if one varies the overlap tolerance from 0.018 to zero, the total energy decreases smoothly to the lower value. Furthermore, increasing the number of zone points used from 19 to 89 changes the energy by 0.000 004 Ry/atom, while decreasing the integral tolerances (see Appendix) by a factor of 100 changes the energy by 0.0001 Ry/atom. In short, the results are internally consistent and numerically stable. The only thing that can be said of this situation is that there appears to be no definitive choice of the overlap tolerance to be made in this instance. For an overlap tolerance of zero, these calculations are 0.02 Ry/atom too low. We do wish to note, however, that the (111) x-ray structure factor for neon is 7.949 for a tolerance of zero, but only changes to 7.953 for a tolerance of 0.014. Similar differences are seen in the other structure factors. The error in the first-order density matrix due to changes in the overlap tolerance is thus small relative to the experimental error in the x-ray structure factors and in the Compton profiles, and to reasonable variations in the Gaussian basis sets.

TABLE VI. Neon and LiF total energies per cell (TE) in Ry; free-atom total energies (atom TE) in Ry; the virial coefficient (η) which gives the negative ratio of twice the kinetic energy per cell to the potential energy per cell; and the pressure-volume product (pV) in Ry. τ is the overlap tolerance used in the Löwdin orthogonalization. These quantities are given for lattice constants (a) in Å.

	a	τ	TE	Atom TE	η	pV
LiF	3.82	0.0	−214.179 79	···	0.999 71	−0.0418
	3.90	0.0	−214.182 16	···	0.999 45	−0.0785
	4.018 52	0.0	−214.183 38	−213.653 85	0.999 15	−0.1208
	4.10	0.0	−214.180 34	···	0.998 986	−0.1446
	4.2	0.0	−214.179 79	···	0.998 85	−0.1645
Ne	4.52	0.0	−257.0994	−257.0803	0.999 67	−0.0574
	4.52	0.014	−257.073 637	···	0.998 94	−0.1817

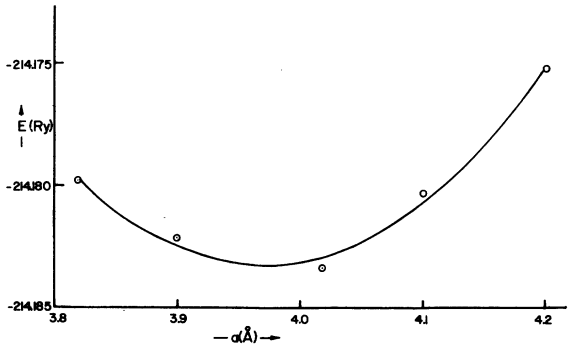

FIG. 1. LiF HF total energy per atom pair in Ry. is plotted against lattice constants in Å. The five calculated points are circled. The least-squares-fitted parabola is also shown.

The LiF crystalline total energies are plotted against lattice constants in Fig. 1. The least-squares-fit parabola has a minimum at a lattice constant of 3.97 Å, which is close to the experimental value of 4.02 Å (Table V). The same 1% decrease below experimental value was found previously for diamond.[2] Löwdin,[9] in a much earlier calculation, found the equilibrium lattice constant of LiF to be 4.2 Å.

The bulk modulus B can be obtained from the curvature of the parabola. For a face-centered-cubic lattice

$$B=\left(\frac{4}{9a}\right)\frac{d^2u}{da^2}\ .$$

Our LiF result of 7.5×10^{11} dyn/cm^2 is about 10% larger than the experimental value of 6.7×10^{11} dyn/cm^2. Löwdin[9] obtained 7.7×10^{11} dyn/cm^2, in close agreement with our result. The HF bulk modulus obtained for diamond was 5% above the experimental value.[2] This parallels experience with molecular force constants, which are also usually too large in the HF approximation.

Table VI also gives the virial coefficient for each lattice constant. This coefficient, the negative ratio of twice the kinetic energy to the potential energy, is unity for any system in equilibrium when a complete basis set is used for the calculation. A quantitative analysis of this statement when a system is not in equilibrium involves the pressure-volume product.[16] For a face-centered crystal

$$pV=\tfrac{1}{3}(2T+V)=-B(3a^2/4)\delta a\,,$$

where T and V are the kinetic and potential energies per cell. The slope and intercept of the pV-vs-a line should again give the HF equilibrium lattice constant and bulk modulus. However, as can be seen from Table VII, the results are bad, as they also were for diamond.[2] Only for a more complete local basis set will the pV analysis give reliable results.

The analysis involving the total energy versus lattice constant, however, does seem reliable for both LiF and diamond. The success in computing the ionic binding energy of LiF, and the equilibrium lattice constant and bulk modulus of LiF and diamond, illustrates the ability of the HF approximation to reproduce the ground state energetics, at least for small symmetric deviations of the atoms from equilibrium.

TABLE VII. LiF experimental and computed equilibrium lattice constants a (Å); bulk modulus B ($\times10^{11}$ dynes/cm^2); and ionic binding energy (IBE) (Ry/pair). The row labeled TE was obtained by analyzing the total energy versus lattice constant curve. The row labeled pV was obtained by analyzing the pV vs lattice constant curve. The Löwdin results are from Ref. 9.

	a	B	IBE
Expt.	4.02	6.71	0.79
TE	3.972	7.54	0.82
pV	3.668	5.89	···
Löwdin	4.2	7.7	0.71

V. X-RAY STRUCTURE FACTORS

The electron charge density $n(r)$ is the diagonal part of the first-order density matrix

$$n(\vec{r})=\rho_1(\vec{r},\vec{r})\,.$$

The Fourier transform of the charge density

TABLE VIII. LiF experimental and calculated structure factors in electrons per unit cell. The experimental values are taken from Ref. 11. The Debye-Waller corrections were removed. The reciprocal-lattice vectors are labeled by the integers h, k, and l.

	LiF		Ne
hkl	Expt.	Calc.	Calc.
111	4.84	4.98	7.95
200	7.74	7.70	7.43
220	5.71	5.72	5.86
311	2.37	2.36	5.05
222	4.61	4.60	4.82
400	3.99	3.90	4.10
331	1.65	1.63	3.69
420	3.46	3.40	3.57
422	3.07	3.04	3.18
511	1.38	1.37	2.94
333	1.38	1.36	2.94
440	2.58	2.57	2.64
531	1.28	1.26	2.49
600	2.41	2.41	2.45
442	2.41	2.41	2.44
620	2.24	2.28	2.29

TABLE IX. Atomic and crystalline HF Compton profiles for neon and crystalline experimental (Ref. 18) and HF Compton profiles for LiF. Huzinaga's 11*s*/7*p* Gaussian basis (Ref. 8) was used for the atomic neon calculation. No eigenvectors of the overlap matrix were discarded in the crystalline calculation. The Compton profiles and momentum transfer q are in atomic units. The column headings (hkl) indicate the direction of the momentum transfer in the crystal.

	Ne	LiF						
q	Atom	100	110	111	Expt.	100	110	111
0.0	2.723	2.722	2.722	2.726	3.78	3.839	3.875	3.881
0.1	2.715	2.716	2.717	2.720	3.74	3.825	3.861	3.865
0.2	2.692	2.695	2.697	2.699	3.70	3.779	3.814	3.818
0.3	2.651	2.654	2.656	2.656	3.59	3.700	3.732	3.740
0.4	2.592	2.593	2.593	2.588	3.47	3.586	3.617	3.630
0.5	2.514	2.513	2.510	2.507	3.31	3.446	3.472	3.488
0.6	2.416	2.413	2.410	2.415	3.12	3.290	3.303	3.315
0.7	2.302	2.296	2.296	2.307	2.91	3.122	3.112	3.113
0.8	2.173	2.167	2.172	2.176	2.71	2.938	2.900	2.887
0.9	2.035	2.030	2.040	2.032	2.48	2.728	2.669	2.646
1.0	1.892	1.889	1.900	1.884	2.22	2.489	2.425	2.398
1.2	1.607	1.607	1.606	1.603	1.75	1.968	1.935	1.921
1.4	1.344	1.348	1.338	1.348	1.37	1.515	1.506	1.514
1.6	1.117	1.125	1.119	1.123	1.11	1.184	1.183	1.189
1.8	0.927	0.934	0.936	0.933	0.94	0.940	0.954	0.962
2.0	0.771	0.776	0.779	0.775	0.80	0.757	0.786	0.783

$$S(\vec{K}) = \left| \int_V n(\vec{r}) e^{i\vec{K}\cdot\vec{r}}\, d\vec{r} \right| ,$$

evaluated for reciprocal-lattice vectors $\vec{K}$ (the integral vanishes otherwise), are the x-ray structure factors. The integration over V, the crystal volume, keeps the integrals finite and ensures that $S(0)$ gives the total electronic charge per cell in the crystal.

The experimental[17] and theoretical structure factors for LiF, and the theoretical structure factors for Ne, are given in Table VIII. The published experimental values include the Debye-Waller factors, which were removed in order to allow comparison with HF results. The agreement between theory and experiment is usually within the estimated experimental error of 1%. The principle exception is the (111) structure factor. This structure factor most directly reflects the valence charge density and therefore is most sensitive to details of the basis set, and to correlation effects. Nevertheless, the 2% discrepancy is not at all serious.

VI. DIRECTIONAL COMPTON PROFILES

The electron momentum distribution is obtained by separately Fourier transforming the two variables in the first-order density matrix

$$\sigma(\vec{k}, \vec{g}) = \int e^{i\vec{k}\cdot\vec{r}} \rho_1(\vec{r}, \vec{r}') e^{-i\vec{g}\cdot\vec{r}'} d\vec{r}\, d\vec{r}'$$

and then taking the diagonal part

$$\tau(k_x, k_y, k_z) = \sigma(\vec{k}, \vec{k}) .$$

The Compton profile in the impulse approximation for momentum transfer q is then the integral over a plane in k space which corresponds to this momentum transfer. For example, for a momentum transfer q in the z direction, the Compton profile is given by

$$J(q) = \frac{1}{(2\pi)^3} \int_{-\infty}^{\infty} dk_x \int_{-\infty}^{\infty} dk_y\, \tau(k_x, k_y, q) .$$

Calculated HF Compton profiles in the impulse approximation for Ne and LiF are tabulated in Table IX, together with the experimental LiF Compton profile.[18] For ease of comparison of theory and experiment, the LiF results are graphed in Fig. 2. The HF curves are consistently above experimental value at low momentum transfer, as is observed in the atomic calculations; we also found this to be true for diamond. The differences between the experimental and calculated profiles are within the quoted experimental accuracy of 3%.

Although Weiss reported observing no appreciable directional dependence of the LiF Compton profiles, our calculations do show a directional dependence of up to 3% between the [100] and all

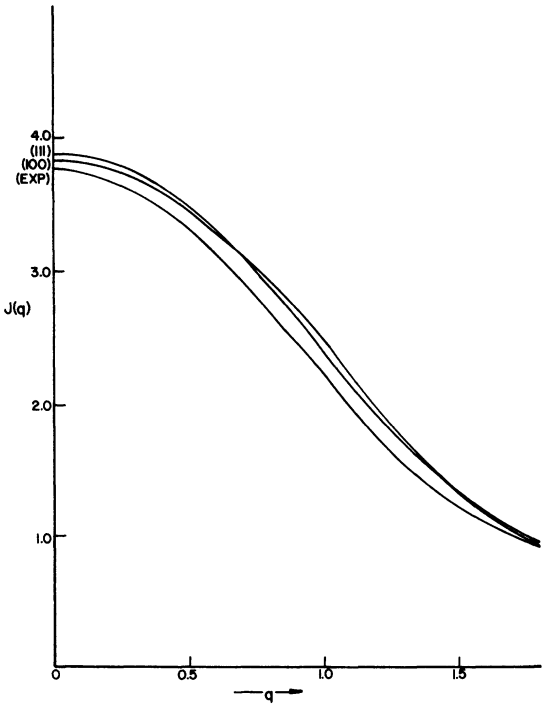

FIG. 2. LiF experimental (Ref. 12) and calculated Compton profiles. Both [111] and [100] directions are shown. Atomic units are used throughout.

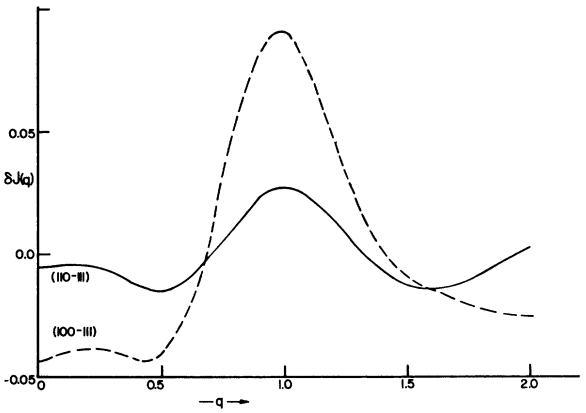

FIG. 3. LiF Compton profile directional dependence is shown. Atomic units are used throughout.

other directions. This dependence is illustrated in Fig. 3. The Compton profiles for the other calculated directions, the [110], [111], [112], and the [221] all agreed with each other to within 1%. The next larger directional dependence is also illustrated in Fig. 3.

The HF Compton profiles for three directions of Ne are also tabulated in Table IX. No appreciable directional dependence was found for the same five calculated directions.

VII. SUMMARY

We have been discussing HF results for a covalent semiconductor, diamond, an ionic insulator, LiF, and a rare-gas insulator, Ne. The remarkably close agreement of our LiF and Ne energy bands with bands obtained by two other completely different computational models gives strong credibility to all three models. The HF equilibrium lattice constant for LiF falls 1% below the experimental value, as does that of diamond. The LiF bulk modulus exceeds the experimental value by 10%, while that of diamond is high by 5%. These results are similar to those obtained from small molecules. We conclude that the HF ground state energetics are relatively close to the experimental values for at least the symmetrical vibrational modes of diamond and LiF.

The HF first-order density matrix results are also good. The x-ray structure factors closely match the experimental values for both diamond and LiF. The agreement of the HF Compton profiles with the experimental values for LiF is somewhat worse than that for diamond,[3] although the LiF results agree to within the quoted experimental uncertainty of 3%. It will be interesting to see whether the predicted directional dependence in the case of LiF is an artifact of the calculation, or is real. The calculated HF directional dependence for diamond is real.[3] The Compton profile for Ne is found to be isotropic, which is consistent with the usual picture of a weakly bound solid of essentially spherical atoms. All of these results indicate that the HF first-order density matrix is quite close to experimental values.

We hope that the success of these crystalline HF calculations will encourage others to join in the development of more efficient HF computational techniques. The HF results are close to experimental values, and can be systematically corrected for correlation effects.

APPENDIX: TREATMENT OF SMALL TWO-ELECTRON INTEGRALS

Two-electron integrals have the form

$$I = \int d\vec{r}\, d\vec{r}\,' \frac{\varphi_1(\vec{r}-\vec{R}_a)\varphi_2(\vec{r}-\vec{R}_b)\varphi_3(\vec{r}\,'-\vec{R}_c)\varphi_4(\vec{r}\,'-\vec{R}_d)}{|\vec{r}-\vec{r}\,'|} .$$

This integral represents the energy of interaction on two charge distributions;

$$I = \int d\vec{r}\, d\vec{r}\,' \frac{n_{12}^{ab}(\vec{r})\, n_{34}^{cd}(\vec{r}\,')}{|\vec{r}-\vec{r}\,'|} .$$

In the first integral approximation,[1,19] the individual $n(\vec{r})$ are each approximated by a single Gaussian for s-s basis pairs, by two Gaussians for s-p pairs, and by four Gaussians for p-p basis pairs. The Gaussian for each lobe-lobe pair has the correct charge and is centered on the center of charge. This approximation is exact when the local basis functions are both single Gaussians, or single Gaussian lobes. All two-electron integrals are first done with this approximation. When the approximate integral is larger than some tolerance (10^{-4}), the integral is redone exactly.

For the two other approximations, we introduce the concept of a "pseudocharge" to measure the "strength" of the charge distribution $n(r)$. For s-s basis pairs, the pseudocharge can be taken as the total charge of the distribution. For s-p and p-p charge distributions, we reorient the p directions to maximize the charge, and we then call this maximal charge the pseudocharge. For basis functions on the same site, we always define the pseudocharge to be unity. In this case,

the s-p total charge is always zero, although the strength of the charge distribution is large. This particular definition has the disadvantage that, for s-p distributions, the pseudocharge is not monotonic, decreasing as the s and p centers move away from each other. There are probably better measures of the strength of charge distributions.

In the second integral approximation,[19] all one- and two-electron integrals are zeroed when the pseudocharge of either distribution is less than some tolerance (10^{-6}). This approximation is also charge conserving, since the first-order density matrix is normalized to the correct charge. Zeroing the one- and two-electron integrals for a given local basis pair eliminates that term from the first-order density matrix.

In the third integral approximation, we make use of the intuitive feeling that integrals involving weak charge distributions with weak charge distributions should be negligible. We thus zero all integrals where the product of the two pseudocharges is less than some tolerance (10^{-4}). We must now restore the lost charge balance. During the self-consistent cycle, we consider each charge distribution of local basis function pairs in turn. We add up the total true charge that this distribution "sees"; i.e., the charge associated with distributions for which the pseudocharge product exceeds the tolerance. We then multiply all nuclear integrals involving this charge distribution by the ratio of the charge observed per cell to the total electronic charge per cell. This scaling of the nuclear integrals again ensures the all-important charge balance.

---

*National Research Council Postdoctoral Fellow, 1972–1973. Present address: Photo Products Dept., Experimental Station, E. I. duPont deNemours and Co., Wilmington, Del. 19898.

[1]R. N. Euwema, D. L. Wilhite, and G. T. Surratt, Phys. Rev. B 7, 818 (1973).
[2]G. T. Surratt, R. N. Euwema, and D. L. Wilhite, Phys. Rev. B 8, 4019 (1973).
[3]G. G. Wepfer, R. N. Euwema, G. T. Surratt, and D. L. Wilhite, Phys. Rev. B (to be published).
[4]A. B. Kunz and D. J. Mickish, Phys. Rev. B 8, 779 (1973).
[5]D. J. Mickish and A. B. Kunz, J. Phys. C 6, 1723 (1973).
[6]L. Dagens and F. Perrot, Phys. Rev. B 5, 641 (1972).
[7]F. Perrot, Phys. Status Solidi 52, 163 (1972).
[8]S. Huzinaga, *Approximate Atomic Functions* (University of Alberta Press, Edmonton, 1971), Vol. I.
[9]P. O. Löwdin, Adv. Phys. 5, 1 (1956).
[10]We are indebted to Professor E. E. Lafon for suggesting this approach.
[11]F. Seitz, *The Modern Theory of Solids* (McGraw-Hill, New York, 1940).
[12]C. Kittel, *Introduction to Solid State Physics*, 3rd ed. (Wiley, New York, 1967).
[13]A. Froman and P. O. Löwdin, J. Phys. Chem. Solids 23, 75 (1962).
[14]J. Linderberg and F. W. Bystrand, Ark. Fys. 26, 383 (1964). A. M. Lesk, J. Chem. Phys. 59, 44 (1973).
[15]G. L. Pollack, Rev. Mod. Phys. 36, 748 (1964).
[16]P. O. Löwdin, J. Mol. Spectrosc. 3, 46 (1959).
[17]M. Merisalo and O. Inkinen, Ann. Acad. Sci. Fenn. A6 207, 3 (1966).
[18]R. J. Weiss, Philos. Mag. 21, 1169 (1970).
[19]D. L. Wilhite and R. N. Euwema, Chem. Phys. Lett. 20, 610 (1973); J. Chem. Phys. (to be published).